

Evaluation of Anti-diabetic Potential of Anti-microbial Carbon Quantum Dots from *Vitis Vinifera* Seeds

C. R. Parvathy, P. K. Praseetha 

Department of Nanotechnology, Noorul Islam Centre for Higher Education, Kumaracoil, India

 Corresponding author. E-mail: crkpkp@gmail.com

Received: Apr. 12, 2022; **Revised:** Dec. 30, 2022; **Accepted:** Feb. 6, 2023

Citation: C.R. Parvathy, P.K. Praseetha. Evaluation of anti-diabetic potential of anti-microbial carbon quantum dots from *vitis vinifera* seeds. *Nano Biomedicine and Engineering*, 2023.

<http://doi.org/10.26599/NBE.2023.9290002>

Abstract

Carbon quantum dots (CQDs) have a size of 10 nm (or less), with lots of biomedical advantages, creating huge excitement in different research fields. The aim of this study includes an eco-friendly synthesis of biogenic CQDs from grape (*Vitis vinifera*) seeds, identifying the characteristics and assessing its anti-diabetic as well as anti-microbial activity. CQDs are prepared by the pyrolysis method. Synthesized CQDs were confirmed by ultraviolet (UV)–visible (Vis) spectrophotometer, and the characterization study was done by X-ray diffractometer, photoluminescence spectroscopy, Fourier transform infra-red spectroscopy, and transmission electron microscopy with selected area electron diffraction (SAED). Anti-diabetic activity of CQDs was analyzed by *in vitro* α -glycosidase, α -amylase inhibition assays, and glucose uptake studies. The anti-bacterial activity of CQDs was analyzed by anti-microbial assay technique against *Escherichia coli*, *Pseudomonas aeruginosa*, *Staphylococcus aureus*, and *Streptococcus mutans*. The results showed that the CQDs synthesized from a natural source like grape seeds, were amorphous in nature, the average particle size was 4 nm, and they contain functional groups like carboxyl and hydroxyl. Subsequently, it showed that the sp² domains also produce green fluorescence. The anti-diabetic experimental method revealed that the CQDs enhance glucose uptake and inhibit carbohydrate hydrolyzing enzymes. CQDs also exhibit anti-bacterial properties against both Gram-positive and Gram-negative bacteria, according to their antimicrobial impact. Due to their small size and higher activity, CQDs will become strong anti-diabetic agents as well as anti-bacterial ones.

Keywords: *Vitis vinifera* seeds; carbon quantum dots (CQDs); green synthesis; anti-bacterial; anti-diabetic activity

Introduction

Scientific and technological expansions gave wonderful opportunities to nanoscience for the synthesis of nanosized carbon structures which completely possess different properties from macroscopic material. Years ago, it was generally hard to accept that carbon was recognized as a black material, which could be soluble in water and even exhibit high fluorescence (FL)

properties. Among the family of carbon nanomaterials, carbon quantum dots (CQDs) are a novel class of nanomaterial, below 10 nm in size [1]. Synthesis methods of CQDs adopted various methods like electrochemical method, chemical route (thermolysis), laser ablation technique, solvothermal method, hydrothermal method, and microwave synthesis. However, green synthesis methods are usually economical, effortless, and safe for the environment [2].

The chemical method shows the presence of some toxic chemicals, and in medical applications sometimes shows hazardous effects. Hence, the newly emerged green chemistry routes are very much needed for the production of eco-friendly and low-cost nanoparticles. The wide range of applications by CQDs in the biomedical and bioimaging field has turned attractive as a prodigious material. Moreover, the scientific community is strongly attracted by CQDs with their unique properties and has received attention for their theranostic applications [3]. Hence in the biomedical field, the unique advantages of these CQDs have gained much more recognition and are involved in a wide range of applications. The present study is hence considered to be novel with the known medical properties of green CQDs.

In Ayurveda, the common grape (*Vitis vinifera*) is known as Draksha. Grape seeds and various parts of grapes are natural substances used for various therapeutic purposes. Today, we know that grape seed contains oligomeric proanthocyanin complex (OPC), an antioxidant that is considered to improve certain diseased conditions. Some scientific evidence indicates that the use of grape seed or its powder reduces poor blood flow in the legs, reduces eye stress due to glare, and is also helpful for reducing high cholesterol and atherosclerosis, and improving athletic performance, heart disease, poor circulation, menopause, diabetes, constipation, gastrointestinal disorders, and macular degeneration due to aging [4].

Grape seed was used in the treatment of diabetes and other age-related diseases [5]. Because anti-diabetic resistance has spread globally, a novel therapeutic agent was very essential to curing diabetic-

related diseases in major treatment, which will also help to replace antibiotics. The nanoparticles that are biogenically synthesized have an anti-diabetic effect, which belong to the molecular drugs of self-functionalization. Hence a better production method has been utilized in the current study for the synthesis of anti-diabetic nanoparticles and is further extended to therapies. So a common medicinal plant, grape, is utilized in this present study. Furthermore, purified and characterized CQDs made from grape seeds were evaluated by different theranostic methods.

Experimental

Collection and preparation of plant material

Healthy, mature, and fresh *Vitis vinifera* belonging to the Vitaceae family was purchased from Parshwa Enterprises (Pune, India). The seeds were rinsed with double distilled water to wash away the undesirable impurities, and particulate suspensions after which shade-dried to be made right into an excellent powder with a digital blender. The powder was stored in a dry and airtight box for further research.

Synthesis of CQDs

CQDs were prepared from 10 g of grape seeds that were kept in an ordinary ceramic crucible at 300 °C for 1 h in a muffle furnace [6]. After that, we obtained dark black products that were cooled all the way down to room temperature and mechanically ground into fine powder with mortar and pestle (Fig. 1). 0.1 g of CQDs were separated and slowly mixed with a magnetic stirrer in 20 mL of distilled water for 20 min. Then, the particles were separated with the help of centrifugation at 4 000 r/min for 30 min.

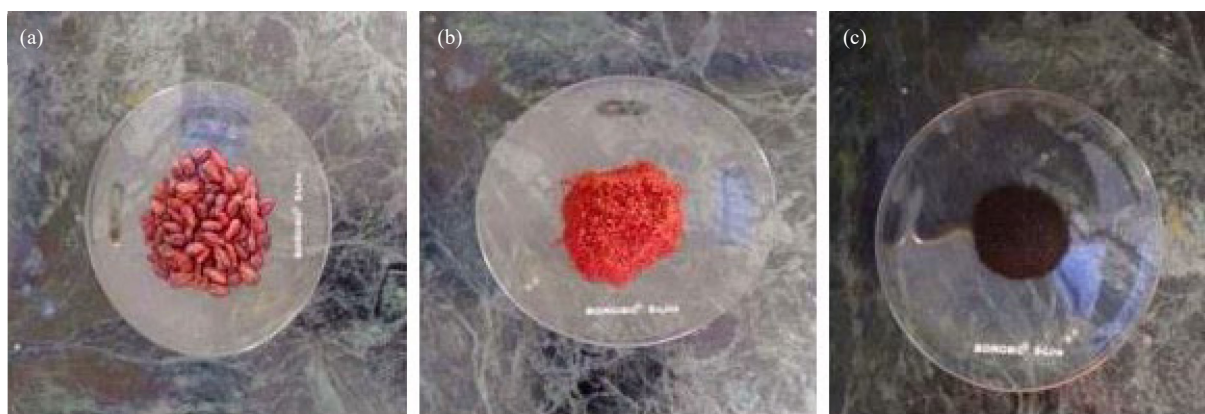


Fig. 1 Visual observation of color changes during the synthesis process: (a) Grape seeds; (b) Fresh powder form of grape seed; (c) Dark black powder (the end product of the pyrolysis method).

Characterization of CQDs

Ultraviolet (UV)–visible (Vis) spectrophotometer (Systronics 2202) was used to measure the UV–Vis absorption spectrum ranging from 300 to 700 nm, and photoluminescence was studied by a fluorescence spectrometer (Jascov-650 spectrophotometer). Powder X-ray diffraction (XRD) of CDQs was recorded by BRUKER D2 Phaser. The use of $K\alpha$ radiation was approximately less than $2\theta - 80^\circ$. Fourier transform infrared spectroscopy (FTIR) (Bruker Alpha T) was used to analyze the functional groups of biogenic CQDs. Transmission electron microscopy (TEM, Hitachi H-7100) also showed the pure elemental CQDs and revealed the nanostructure of the sample.

In vitro α -amylase inhibition assay

CQDs and grape seed were prepared at different concentrations for an α -amylase inhibition assay. Different concentrations of 125–1 000 $\mu\text{g/mL}$ were prepared from a stock concentration of 10 mg/mL along with 25 mmol/L ($\text{pH} = 6.9$) phosphate buffer (25 μL of porcine α -amylase (0.5 mg/mL)) and made up to 1 000 μL , allowed for incubation at 25 $^\circ\text{C}$ for 10 min. 25 mmol/L phosphate buffer ($\text{pH} = 6.9$) and 25 μL of starch solution (0.5%) were added after pre-incubation, then allowed for a second incubation at 25 $^\circ\text{C}$ for 10 min. The coloring agents like 3,5-dinitro salicylic acids were added to stop the reaction.

The microplate was incubated in a boiling water bath for 5 min and then cooled at room temperature. A microplate reader (Erba, Lisascan) was used to measure the absorbance at 540 nm; acarbose was used as standard and the percentage of inhibition was calculated by the formula:

$$\text{Inhibition} = \frac{\text{Control} - \text{Test}}{\text{Control}} \times 100\% \quad (1)$$

In vitro α -glucosidase inhibition assay

10 mg/mL stock concentration of grape seed and CQDs at different concentrations of 125–1 000 $\mu\text{g/mL}$ were prepared and incubated for 5 min. Before initiating the reaction with substrates sucrose (37 mmol/L), 1 mL of phosphate buffer (0.1 mol/L) ($\text{pH} = 7.2$) was reacted as the final reaction mixture and incubated at 37 $^\circ\text{C}$ for 20 and 30 min. After the incubation, the reaction was stopped by boiling the mixture in a water bath for 2 min. Phosphate buffer and enzyme were maintained as control, and acarbose

was used as the standard indicates. 250 μL of glucose reagent was added, followed by incubation for 10 min, and a microplate reader (Erba, Lisascan) was used for measuring absorbance at 510 nm and calculated by Eq.(1).

Evaluation of glucose uptake capacity by yeast cells

A well-defined method [7] was used to perform this assay. For this assay, we prepared 1% yeast suspension, dissolved it in distilled water, then kept it at 25 $^\circ\text{C}$ overnight. After incubation, this yeast cell suspension was centrifuged at 4 200 r/min for 5 min. We got a clean supernatant by adding distilled water and prepared 10% (volume fraction) suspensions of the yeast cells.

We prepared the sample (1–5 mg of the CQDs and mixed with dimethyl sulfoxide (DMSO)) till dissolution. 1 mL of a glucose solution at various concentrations (5, 10, and 15 mmol/L) was added to the sample solution and then incubated for 10 min at 37 $^\circ\text{C}$. After the incubation step to initiate the reaction, 100 μL of yeast suspension was poured into the mixture of glucose and the sample solution was incubated at 37 $^\circ\text{C}$ for 60 min. To estimate the glucose after incubation, the tubes were centrifuged for 5 min at 3 800 r/min . A same wavelength was used to record the absorbance of the control, where except for the test sample, all reagents present in the control solution and metronidazole were used as standard. The glucose uptake was calculated by the formula:

$$\frac{\text{Abs. of control} - \text{Abs. of the sample}}{\text{Abs. of control}} \times 100\% \quad (2)$$

Antimicrobial assay

Antimicrobial property of CQDs was examined by the growth kinetics method using *Vitis vinifera*. In the existing antimicrobial assay, the bacterial concentrations in the presence of CQDs were measured every 2 h after 30 s of agitation to determine bacterial concentrations over time. The antibacterial kinetics was visualized as a graph of contact time against OD_{600} to examine the antigenic property.

Microorganisms like *Escherichia coli* (ATCC 25922), *Pseudomonas aeruginosa* (ATCC 27853), *Staphylococcus aureus* (ATCC 25923), and *Streptococcus mutans* (MTCC 890) received from Microbial Type Culture Collection (MTCC) and

American Type Culture Collection (ATCC) were acquired from Biogenix research Lab (Trivandrum, India).

$$I = \frac{(C_{18} - C_0) - (T_{18} - T_0)}{(C_{18} - C_0)} \times 100\% \quad (3)$$

where I is percentage inhibition of growth, C_{18} is blank-compensated optical density at 600 nm (OD_{600}) of the positive control of the organism at 18 h, C_0 is blank-compensated OD_{600} of the positive control of the organism at 0 h, T_{18} is negative control-compensated OD_{600} of the organism in the presence of the test sample at 18 h, and T_0 is negative control-compensated OD_{600} of the organism in the presence of the test sample at 0 h.

Results and Discussion

UV absorption and PL spectrum studies

A simple and most outstanding evaluating technique for CQDs was UV–Vis absorption studies. This characterization study was done at a wavelength range of 200–600 nm. The huge UV peak of CQDs was found in the UV region at 262 nm as represented in Fig. 2(a). The PL spectrum of CQDs in Fig. 2(b) shows that a broad peak in excitation and emission wavelengths reaches the peaks at 380 and 540 nm, respectively.

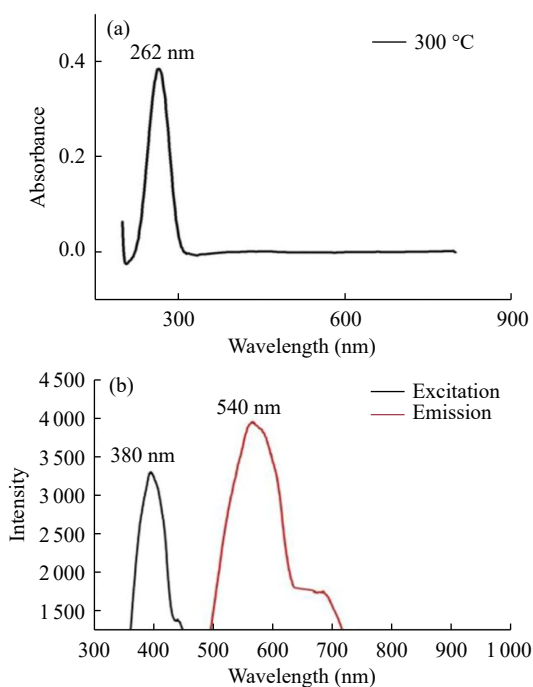


Fig. 2 (a) UV–Vis spectra represents the formation of CQDs by *Vitis vinifera* seed; (b) PL spectrum (emission and excitation) of CQDs.

The absorbance spectra of CQDs have been recorded within 210–320 nm. Our research supported the view that the C=O band is due to the $n \rightarrow \pi^*$ transition by the above findings [8]. The excitation and emission wavelength of CQDs were increased from 330 to 490 nm and from 430 to 590 nm, respectively. When the excitation wavelength increases, the existence of photon re-absorption and the fluorescence emitting peaks convert to redshift. The result reveals that CQDs also show the green fluorescence that is identified with the quantum-confinement effect and edge defects [9].

XRD method

A rapid structural analytical method of biogenic CQDs was recorded by the XRD method in the range of $10^\circ < 2\theta < 80^\circ$. In the XRD spectra, strong diffraction peaks of CQDs were displayed at 23.8° (Fig. 3) corresponding to (002) plane. The average crystalline size of the prepared nanoparticles was calculated by Debye Scherrer's formula: $D = 0.9\lambda/(\beta\cos\theta)$, where D is crystallite size, λ is the wavelength of X-ray (1.5406 \AA), β is the full width at half maximum (FWHM), and θ denotes the Bragg's angle. The average particle size of the prepared CQD was 1.165 nm in diameter and was correlated with the TEM micrograph of green synthesized CQDs. XRD patterns are broad; the diffraction peak shows that the synthesized nanoparticles are amorphous and pure [10].

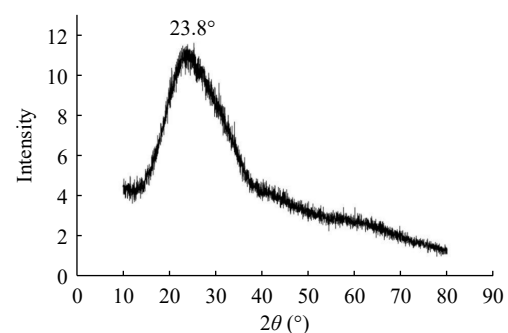


Fig. 3 XRD graph represents the amorphous nature of CQDs.

FTIR method

Possible and different functional groups involved in CQDs were identified with the help of FTIR analysis. FTIR spectrum range of grape seed CQDs was $500\text{--}4000 \text{ cm}^{-1}$ (Fig. 4).

The 1521 cm^{-1} peak attributed to the C=C stretch, i.e., unsaturated alkenes. A peak at 1732 cm^{-1} was the

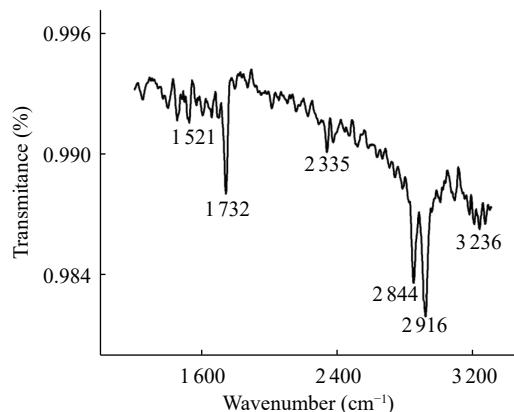


Fig. 4 FTIR graph represents the functional groups present on the surface of CQDs.

stretching of the C=O bend representing the primary carboxyl compound. The band at 2844 and 2916 cm^{-1} stretching was attributed to being a C—H bond. The 2335 cm^{-1} peak was due to the presence of COO^- . The C—OH group was attributed to being a band at 3236 cm^{-1} . The results explain that the carboxyl hydroxyl, and oxygen-containing groups are present in the CQDs. Aqueous solubility of CQDs contributed to all these functional groups after dehydration or carbonization that leads to the sp^2 domains and these are derived from small precursor molecules such as glucose, fructose, and ascorbic acid. Therefore, the formation of the CQDs contributes to split bonds to the surrounding oxygen groups [11–13].

Microscopic analysis TEM with selected area electron diffraction pattern (SAED)

TEM micrograph with SAED pattern confirmed that the average particle size of CQDs was measured as 4 nm (Figs. 5(a) and 5(b)). XRD values were well supported by the result. Characterized TEM images indicate that spherical-shaped CQDs are found on the sample. SAED shows that prepared biogenic CQDs are highly amorphous.

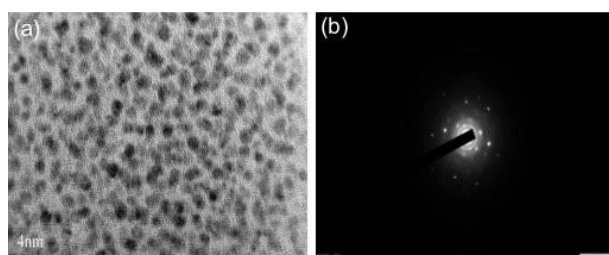


Fig. 5 (a) TEM image indicates the spherical-shaped CQDs; **(b)** SAED pattern of CQDs confirms highly amorphous nature.

Anti-diabetic Analysis

In vitro carbohydrate-hydrolyzing enzyme assays

CQDs are effectively inhibited by carbohydrate-hydrolyzing enzymes like α -amylase and α -glucosidase. Increasing the concentration of CQDs influences the enzymatic activity level. IC_{50} values (α -amylase and α -glucosidase) for grape seed CQDs inhibition were 55.5 and 51.7 $\mu\text{g/mL}$, respectively (Figs. 6(a) and 6(b)). The digestive tract contains two types of enzymes like α -amylase and α -glucosidase. Both carbohydrate-hydrolyzing enzymes manage the absorption by breaking down carbohydrates into monosaccharides. Grape seed CQDs exhibit inhibition for digestive tract enzymes. Grape seed contains some photochemicals; these are attached to CQDs and give a superior activity mechanism to anti-diabetic potential compared with grape seed [14,15]. The use of biological CQDs can make the treatment of diabetes and the complications easier. Amylase and glucosidase enzymes break down carbohydrates and raise blood sugar levels in diabetics. These two enzymes can be inhibited to regulate diabetes and lower the chance of getting it. Availability of CQDs that inhibit α -amylase and α -glucosidase, however, is

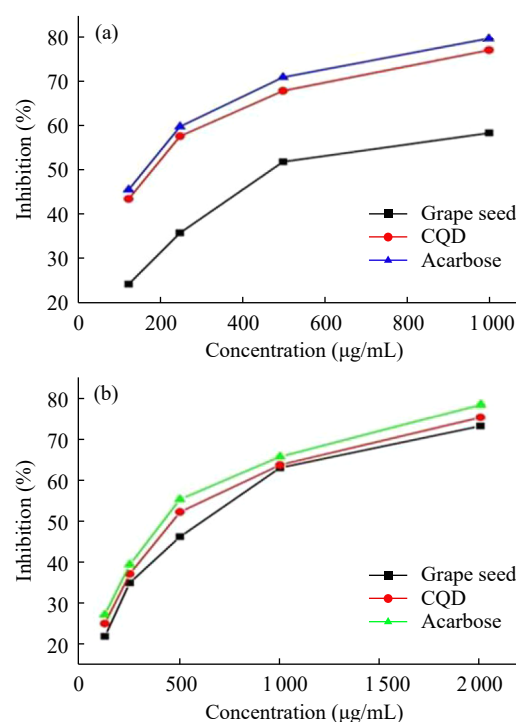


Fig. 6 Graph represents anti-diabetic activity in terms of inhibition of carbohydrate hydrolyzing enzymes: **(a)** *In vitro* α -amylase inhibition assay by CQDs, grape seed, and standard acarbose; **(b)** α -glucosidase inhibition assay by CQDs, grape seed, and standard acarbose.

well known. It protects against diabetes by reducing the anti-inflammatory activity linked to diabetics, controlling glucosidase and amylase, and improving insulin sensitivity and pancreatic function.

Effect of CQDs on glucose uptake capacity by yeast cells

Green synthesized CQDs help to increase the glucose uptake in the yeast cells in which water acts as a control. A colorimetric method was used to identify the presence of unused glucose, which was helpful to evaluate the amount of glucose uptake capacity in the yeast cell. Figure 7 shows the rate of glucose uptake in the yeast cells. When the sample amount increases glucose, uptake decreases with reducing glucose concentration.

Based on the general concept of glucose uptake, glucose-transporting molecules assemble in the cell membrane by skeletal muscles. In the hypoglycemic effect, leptocytes and/or myocytes regulate glucose-transporting molecules that lead to the high secretion of insulin in the blood. Yeast cells show a difference in glucose uptake from that of other cells. In the yeast membrane, the glucose uptake is taking place by a different process like the phosphotransferase enzyme system and facilitated diffusion. In glucose uptake, different variables affect glucose concentration and subsequent metabolism of glucose inside the yeast cells. The internal glucose concentration in the cell influences the glucose uptake when most of the internal sugar is converted simply into different metabolites. In the present study, because of the facilitated diffusion and elevated glucose metabolism, the CQDs could bind glucose effectively and also enhance the body's muscle cells and adipose tissues during transport across the cell membrane [16, 17].

Antimicrobial analysis

Biosynthesized CQDs were analyzed by different strains of bacterial cultures. As the concentration of CQDs increases, its antibacterial activity equally increases. Overall growth kinetics of four microbes *S. aureus*, *S. mutans*, *E. coli*, and *P. aeruginosa* have been investigated in this study. At 80 $\mu\text{g/mL}$, CQDs inhibit the growth of *S. aureus*, *S. mutans*, and *E. coli* by up to 50%, 30%, and 30%, respectively, and the inhibition is over 90% for these three at 100 $\mu\text{g/mL}$.

However, CQDs slightly inhibit the development

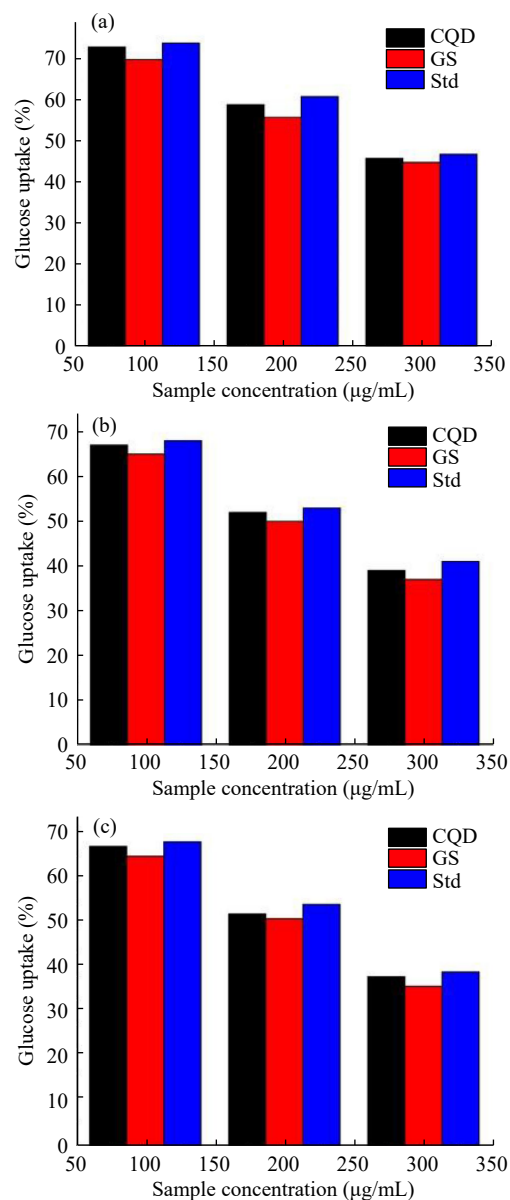


Fig. 7 Rate of glucose uptake in the yeast cells (Glucose concentrations (5, 10, and 15 mmol/L) in the presence of CQDs, grape seed, and metronidazole as standard (Std)): (a) Glucose concentration (5 mmol/L); (b) Glucose concentration (10 mmol/L); (c) Glucose concentration (15 mmol/L).

of *P. aeruginosa* in both doses. As the result shows, investigation of the growth kinetics of bacteria is the most effective method for determining the antibacterial activity of CQDs (Fig. 8). The underlying molecular mechanism of such antibacterial activities of CQDs has been thoroughly studied. The impact of the CQDs was found to be much stronger in Gram-positive bacteria than in Gram-negative ones. We assume the CQDs increased antibacterial impact is due to their persistence as a colloid in the medium, which alters the phosphotyrosine profile of bacterial proteins and stops bacterial growth.

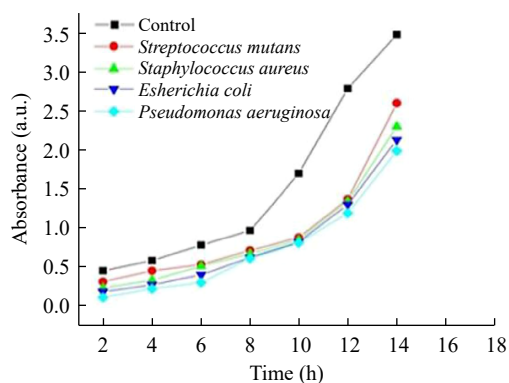


Fig. 8 CQDs have anti-bacterial activity against *S. aureus*, *S. mutans*, *P. aeruginosa*, *E. coli*, and control at 100 $\mu\text{g/mL}$.

Conclusion

The biogenic CQDs synthesis procedure was an advanced approach to an eco-friendly, biogenic, and cost-effective synthesis from grape seed. Synthesized particles were characterized by UV–Vis absorption peak at 262.4 nm, XRD, FTIR, and TEM. Organic phytochemicals including phenolic acids, anthocyanins, flavonoids, and one of the best-known sources of oligomeric proanthocyanidin complexes (OPCs) are present in grape seed. There should be an easy, effective, safe and new technique for the biosynthesis of anti-diabetic CQDs. This approach also has great applicability due to low toxicity, economic viability and usage of economically important plants, which further leads to theranostic applications.

CRedit Author Statement

C. R. Parvathy: Analyze synthesis and characterization, monitor CQDs activities, writing and editing. **P. K. Praseetha:** Design and supervise the work.

Conflict of Interest

The authors declare that they have no conflicts of interest to disclose.

References

[1] M. Sundrarajan, S. Ambika, K. Bharathi. Plant-extract mediated synthesis of ZnO nanoparticles using *Pongamia pinnata* and their activity against pathogenic bacteria. *Advanced Powder Technology*, 2015, 26(5): 1294–1299. <https://doi.org/10.1016/j.apt.2015.07.001>

[2] R. Yuvakkumar, J. Suresh, A.J. Nathanael, et al. Novel green synthetic strategy to prepare ZnO nanocrystals using rambutan (*Nephelium lappaceum* L) peel extract and its antibacterial applications. *Materials Science and Engineering: C*, 2014, 41: 17–27. <https://doi.org/10.1016/j.msec.2014.04.025>

[3] S. Yedurkar, C. Maurya, P. Mahanwar. Biosynthesis of zinc oxide nanoparticles using *Ixora coccinea* leaf extract—A green approach. *Open Journal of Synthesis Theory and Applications*, 2016, 5: 1–14. <https://doi.org/10.4236/ojsta.2016.51001>

[4] <https://www.verywellhealth.com/the-benefits-of-grape-seed-extract-89055>

[5] R.S. Sanna, S. Muthangi, B.K. CS, et al. Grape seed proanthocyanidin extract and insulin prevents cognitive decline in type 1 diabetic rat by impacting Bcl-2 and Bax in the prefrontal cortex. *Metabolic Brain Disease*, 2019, 34(1): 103–117. <https://doi.org/10.1007/s11011-018-0320-5>

[6] A. Chatzimakou, T.G. Chatzimitakos, A. Kasouni, et al. Selective FRET-based sensing of 4-nitrophenol and cell imaging capitalizing on the fluorescent properties of carbon nanodots from apple seeds. *Sensors and Actuators B: Chemical*, 2018, 258: 1152–1160. <https://doi.org/10.1016/j.snb.2017.11.182>

[7] V.P. Cirillo. Mechanism of glucose transport across the yeast cell membrane. *Journal of Bacteriology*, 1962, 84: 485–491. <https://doi.org/10.1128/jb.84.3.485-491.1962>

[8] N.A. Alarfaj, M.F. El-Tohamy, H.F. Oraby. CA 19-9 pancreatic tumor marker fluorescence immunosensing detection via immobilized carbon quantum dots conjugated gold nanocomposite. *International Journal of Molecular Sciences*, 2018, 19(4): E1162. <https://doi.org/10.3390/ijms19041162>

[9] Y.F. Wang, A.G. Hu. Carbon quantum dots: Synthesis, properties and applications. *Journal of Materials Chemistry C*, 2014, 2(34): 6921–6939. <https://doi.org/10.1039/C4TC00988F>

[10] R. Atchudana, T. Nesakumar Jebakumar Immanuel Edison, M.G. Sethuraman. Efficient synthesis of highly fluorescent nitrogen-doped carbon dots for cell imaging using unripe fruit extract of *Prunus mume*. *Applied Surface Science*, 2016, 384: 432–441. <https://doi.org/10.1016/j.apsusc.2016.05.054>

[11] F.S. Wu, H.F. Su, K. Wang, et al. Facile synthesis of N-rich carbon quantum dots from porphyrins as efficient probes for bioimaging and biosensing in living cells. *International Journal of Nanomedicine*, 2017, 12: 7375–7391. <https://doi.org/10.2147/IJN.S147165>

[12] M. He, J. Zhang, H. Wang, et al. Material and optical properties of fluorescent carbon quantum dots fabricated from lemon juice via hydrothermal reaction. *Nanoscale Research Letters*, 2018, 13(1): 175. <https://doi.org/10.1186/s11671-018-2581-7>

[13] L.A.A. Chunduri, A. Kurdekar, S. Patnaik, et al. Single step synthesis of carbon quantum dots from coconut shell: Evaluation for antioxidant efficacy and hemotoxicity. *Journal of Materials Sciences and Applications*, 2017, 3(6): 83–93.

[14] X. Chen, J. Xiong, Q. He, et al. Characterization and potential antidiabetic activity of proanthocyanidins from the barks of *Acacia mangium* and *Larix gmelinii*. *Journal of Chemistry*, 2019, 2019: 4793047. <https://doi.org/10.1155/2019/4793047>

[15] R.G. Saratale, H.S. Shin, G. Kumar, et al. Exploiting antidiabetic activity of silver nanoparticles synthesized using *Punica granatum* leaves and anticancer potential

- against human liver cancer cells (HepG2). *Artificial Cells, Nanomedicine, and Biotechnology*, 2018, 46(1): 211–222. <https://doi.org/10.1080/21691401.2017.1337031>
- [16] V. Vishnupriyan, R. Arulvel, S. Rajeswari, et al. Antidiabetic and antioxidant activity of green synthesized starch nanoparticles: An in vitro study. *Journal of Cluster Science*, 2020, 31: 1257–1266. <https://doi.org/10.1007/s10876-019-01732-3>
- [17] C.Y. Wong, H. Al-Salami, C.R. Dass. Formulation and characterization of insulin-loaded chitosan nanoparticles capable of inducing glucose uptake in skeletal muscle cells *in vitro*. *Journal of Drug Delivery Science and Technology*, 2020, 57: 101738. <https://doi.org/10.1016/j.jddst.2020.101738>

© The author(s) 2023. This is an open-access article distributed under the terms of the Creative Commons Attribution 4.0 International License (CC BY) (<http://creativecommons.org/licenses/by/4.0/>), which permits unrestricted use, distribution, and reproduction in any medium, provided the original author and source are credited.